Available online at www.sciencedirect.com

ScienceDirect

Ceramics International 40 (2014) 2173–2178

CERAMICS INTERNATIONAL

www.elsevier.com/locate/ceramint

Photoluminescence properties of Eu^{3+} in garnet-type $Li_7La_3Zr_2O_{12}$ polycrystalline ceramics

Xinmin Zhang[a,c,*], Zhongfeng Zhang[b], Sun Il Kim[c], Young Moon Yu[d], Hyo Jin Seo[c]

[a]School of Materials Science and Engineering, Central South University of Forestry and Technology, Changsha 410004, China
[b]Department of Furniture, Central South University of Forestry and Technology, Changsha 410004, China
[c]Department of Physics and Interdisciplinary Program of Biomedical Engineering, Pukyong National University, Busan 608-737, Republic of Korea
[d]LED-Marin Convergence Technology R&BD Center, Pukyong National University, Busan 608-739, Republic of Korea

Received 4 July 2013; received in revised form 19 July 2013; accepted 28 July 2013
Available online 2 August 2013

Abstract

Novel Eu^{3+} doped zirconate garnet-type ceramics, $Li_7(La_{3-x}Eu_x)Zr_2O_{12}$ with $x=0$, 0.001–1.0, have been synthesized by solid state reaction and the purity phase of the samples was checked by XRD. Room temperature steady and time-resolved emission spectra, under UV and visible light excitation energy, have been investigated. The concentration effect on the quenching blue emission, due to the Zr–O charge transfer transition and $^5D_0 \rightarrow {}^7F_2$ emission transition of Eu^{3+} were studied in detail. The results indicate that there exists efficient energy transfer from host to Eu^{3+}. The mechanism of interaction between Eu^{3+} ions has also been investigated by means of the Inokuti–Hirayama model.

Keywords: A. Powder: solid state reaction; B. Spectroscopy; C. Optical properties

1. Introduction

Rare earth ions activated phosphors exhibit excellent optical properties. They have a wide variety of applications in the fields of lighting, display, laser, scintillator, and amplifiers for fiber-optic communications, etc [1]. The recent developments of solid state lighting have attracted more attention in searching for novel efficient inorganic luminescent materials [2–4]. Especially, investigation of luminescence properties of Eu^{3+} ions in various host lattices is of immense interest both from scientific and technological points of view [5–7]. Indeed Eu^{3+} ions are stable at ambient conditions and exhibit a narrow band emission due to the *f–f* transitions.

Among the various lattices studied, the molybdates, tungstates, vanadates and phosphates have been reported to be good phosphor hosts [8–12]. Zirconates are characterized with high melting point, low thermal conductivity, high thermal expansion coefficient, high chemical stability, and so on. They have wide applications in the fields of refractory, thermal barrier coating material and solid electrolyte material [13,14]. However, the optical properties of zirconates and rare earth ions activated zirconates have not been studied extensively [15,16].

Usually, the luminescence properties reported in zirconates host are due to the Zr–O charge transfer transition. The Zr^{4+}-related emissions were reported in $Ca_3ZrSi_2O_9$ and Sr_2ZrO_4 at low temperature [17,18]. However, the visible Zr^{4+}-related emission at room temperature has been rarely reported [19].

In this paper, we report the Zr^{4+}-related emission in the visible region and the energy transfer from host to Eu^{3+} ions in novel $Li_7(La_{3-x}Eu_x)Zr_2O_{12}$ phosphors. The mechanism of interaction between Eu^{3+} ions is also investigated by means of the Inokuti–Hirayama model.

2. Experimental

$Li_7(La_{3-x}Eu_x)Zr_2O_{12}$ phosphors were prepared by high temperature solid state reaction. Raw materials Li_2CO_3 (excess

*Corresponding author. Postal address: College of Materials Science and Engineering, Central South University of Forestry and Technology, Changsha 410004, China. Tel.: +86 731 85623303; fax: +86 731 85623303.
E-mail addresses: zhxmuga@163.com (X. Zhang), hjseo@pknu.ac.kr (H.J. Seo).

0272-8842/$ - see front matter © 2013 Elsevier Ltd and Techna Group S.r.l. All rights reserved.
http://dx.doi.org/10.1016/j.ceramint.2013.07.135

20 mol% to compensate the evaporation), La_2O_3, Eu_2O_3, and ZrO_2 (all materials are bought from Aldrich, 99.99%) were thoroughly mixed in an agate mortar. The sintering process consists of two steps: the first step is at 900 °C for 5 h, and the second step is at 980 °C for 5 h. Both steps are carried out at air atmosphere. X-ray powder diffraction (Beijing Puxi, XD-2, Cu Kα, $\lambda = 1.5405$ Å) was used to identify the structure of the final product. Excitation and emission spectra were carried out by a fluorescence meter (Shimadzu, RF 5301PC) with a 150 W Xe lamp as an excitation source. The decay curves were recorded by the 500 MHz digital storage oscilloscope (LeCroy 9350 A) in which the signal was fed from PMT. The samples were excited by 266 nm UV laser. All measurements were carried out at room temperature.

3. Results and discussion

The selected powder XRD patterns of $Li_7(La_{3-x}Eu_x)Zr_2O_{12}$ phosphors are shown in Fig. 1. $Li_7La_3Zr_2O_{12}$ has a garnet type crystal structure that has two stable phases: tetragonal phase and cubic phase. A close inspection of the patterns has revealed that the peaks shown in Fig. 1(b), (c) and (d) are consistent with that of JCPDS 80-0457 [Fig. 1(a)] [20], indicating that these samples have cubic crystal structure and the doped Eu^{3+} ions can substitute for the cations sites without disturbing the host′s structure. In this case, the doped Eu^{3+} should replace the La^{3+} sites if the charge and radius of ions are taken into consideration. When $x \geq 2.0$ the XRD patterns of samples cannot be indexed to either tetragonal or cubic $Li_7La_3Zr_2O_{12}$, which could be attributed to the radius difference between Eu^{3+} and La^{3+} ions resulting in the different crystal structure. The influence on crystal structure at higher doped concentration is under investigation.

Under 254 nm UV lamp radiation, undoped $Li_7La_3Zr_2O_{12}$ gives a blue emission. The emission and excitation spectra of undoped $Li_7La_3Zr_2O_{12}$ are shown in Fig. 2. It is found that the host lattice emission occurs as a broad band peaking at 430 nm. Considering the garnet type crystal structure of $Li_7La_3Zr_2O_{12}$, constituted by dodecahedral LaO_8 and octahedral ZrO_6 [21]. The emission at 430 nm can be attributed to the Zr–O charge transfer transition. Broad UV–visible emissions have been reported in compounds with tetravalent (M^{4+}) cations such as Zr^{4+} [17], Ce^{4+}[22], and Ti^{4+} [23] in which the M^{4+}–O^{2-} charge transfer (M–O CT) transition is responsible for the emissions. The M–O CT transition takes place uniquely from the M^{4+} ions with octahedral coordination of oxygen ions [19]. The excitation band obtained by monitoring the 430 nm emission has a maximum at around 247 nm. The decay curve of blue emission under pulsed laser excitation ($\lambda = 266$ nm) is shown in the inset of Fig. 2. It can be seen that the decay curve is non-exponential. The average decay time has been estimated by means of the formula [24]

$$\tau = \frac{\int tI(t)dt}{\int I(t)dt} \quad (1)$$

where $I(t)$ represents the luminescence intensity at time t. The derived τ is about 4.08 μs.

The excitation and emission spectra of $Li_7(La_{2.70}Eu_{0.30})Zr_2O_{12}$ sample are shown in Fig. 3. The excitation spectrum consists of a broad band peaking at 277 nm and sharp peaks in the range of 350–550 nm. Compared to the excitation spectrum shown in Fig. 2, the broad band in Fig. 3 shifts to lower energy, which may attribute to the overlap of charge transfer absorption from the O^{2-} ligands to the d orbitals of the Zr and the f orbitals of the Eu ions. The sharp peaks originate from the transitions with the f-configuration from $^7F_0$ to the excitation states.

The emission spectra when excited by different light are dominated by the two transitions of $^5D_0 \rightarrow {}^7F_1$ (588 nm) and $^5D_0 \rightarrow {}^7F_2$ (608 nm). It is well known that $^5D_0 \rightarrow {}^7F_1$ is a magnetic dipole transition in nature and is also independent of the crystallographic site of the Eu^{3+} ions. $^5D_0 \rightarrow {}^7F_2$ is an electric dipole transition and the intensity is stronger than that of magnetic dipole transition. This indicates that Eu^{3+} ions occupy the non-centrosymmetric sites and is consistent with

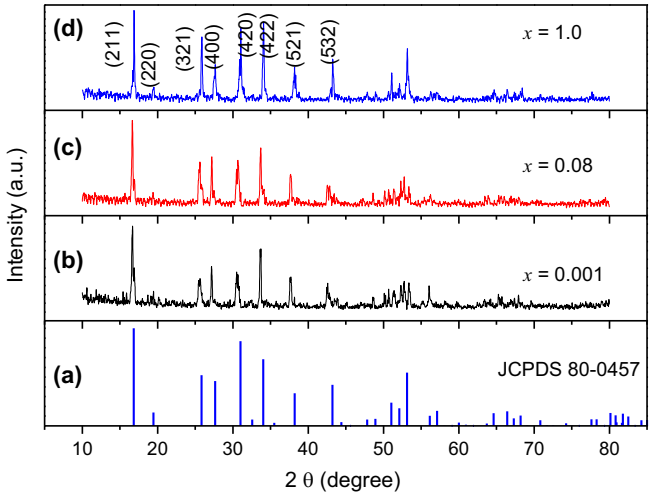

Fig. 1. XRD patterns of $Li_7(La_{3-x}Eu_x)Zr_2O_{12}$ samples with different Eu^{3+} concentration.

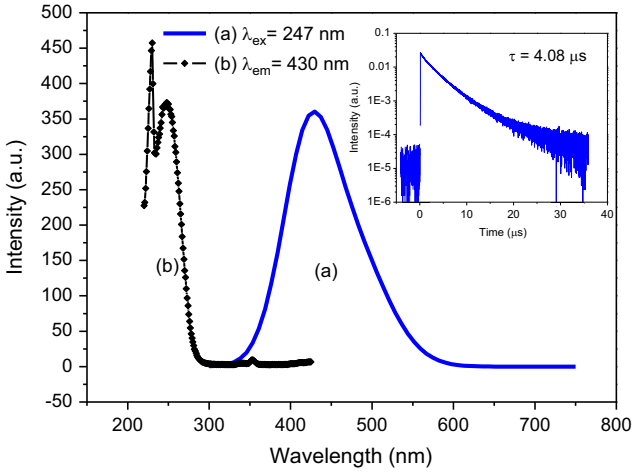

Fig. 2. (a) Emission ($\lambda_{ex} = 247$ nm) and (b) excitation spectra ($\lambda_{em} = 430$ nm) of $Li_7La_3Zr_2O_{12}$. The inset shows the decay curve of blue emission band in undoped $Li_7La_3Zr_2O_{12}$. (For interpretation of the references to color in this figure legend, the reader is referred to the web version of this article.)

analysis of crystal structure [20,25]. It is noted that in $Li_7(La_{2.70}Eu_{0.30})Zr_2O_{12}$ sample the host emission does not appear when excited by UV radiations (247 nm, corresponding to the host absorption), which is not consistent with the emission spectrum in Fig. 2. The result could be attributed to the energy transfer process from host to Eu^{3+}.

In order to investigate the energy transfer behavior from host to Eu^{3+} in $Li_7La_3Zr_2O_{12}$:Eu^{3+}, the emission spectra of $Li_7La_3Zr_2O_{12}$:Eu^{3+} with different Eu^{3+} concentrations were measured and the results are shown in Fig. 4. It can be seen that both the host emission and Eu^{3+} emission are observed at lower Eu^{3+} concentration. The intensity of host emission band decreases as the Eu^{3+} dopants are increased; while the intensity of Eu^{3+} emission increases when Eu^{3+} concentration is up to $x=0.30$, and then decreases because of concentration quenching (see detail in the inset of Fig. 4). This phenomenon suggests that energy transfer takes place from host to Eu^{3+}. At the same time we observe that quenching of emission intensity occurs when x exceeds 0.30. So the critical distance for energy transfer (R_c) can be calculated using the equation proposed by Blasse [26]

$$R_c \approx 2\left(\frac{3V}{4\pi x_C N}\right)^{1/3} \quad (2)$$

where x_c is the critical concentration of the activator ion, N is the number of the center cations ions in the unit cell, and V is the volume of the unit cell. In $Li_7La_3Zr_2O_{12}$, $V=2145.39$ Å^3

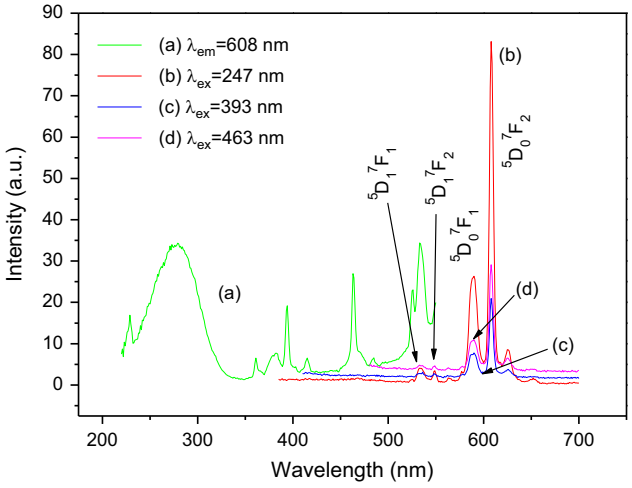

Fig. 3. (a) Excitation ($\lambda_{em}=608$ nm) and (b, c, and d) emission ($\lambda_{ex}=247$, 393 and 463 nm) spectra of $Li_7(La_{2.70}Eu_{0.30})Zr_2O_{12}$ sample.

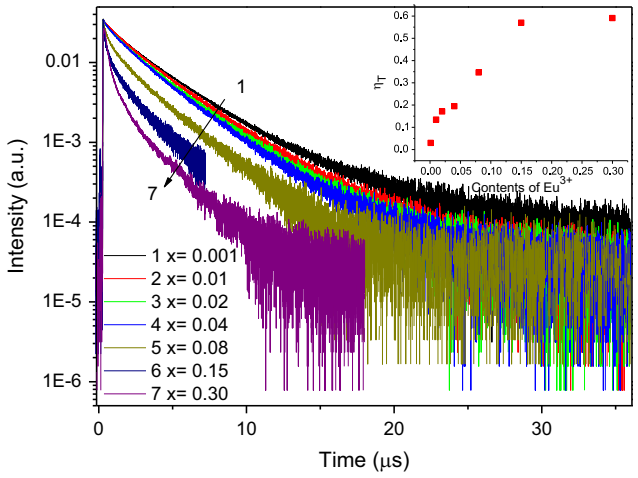

Fig. 5. Eu^{3+} concentration dependence of decay curves of host emission ($\lambda_{ex}=266$ nm, $\lambda_{em}=430$ nm) for $Li_7(La_{3-x}Eu_x)Zr_2O_{12}$ phosphors. The inset shows the energy transfer efficiency from host to Eu^{3+} in $Li_7(La_{3-x}Eu_x)Zr_2O_{12}$ samples.

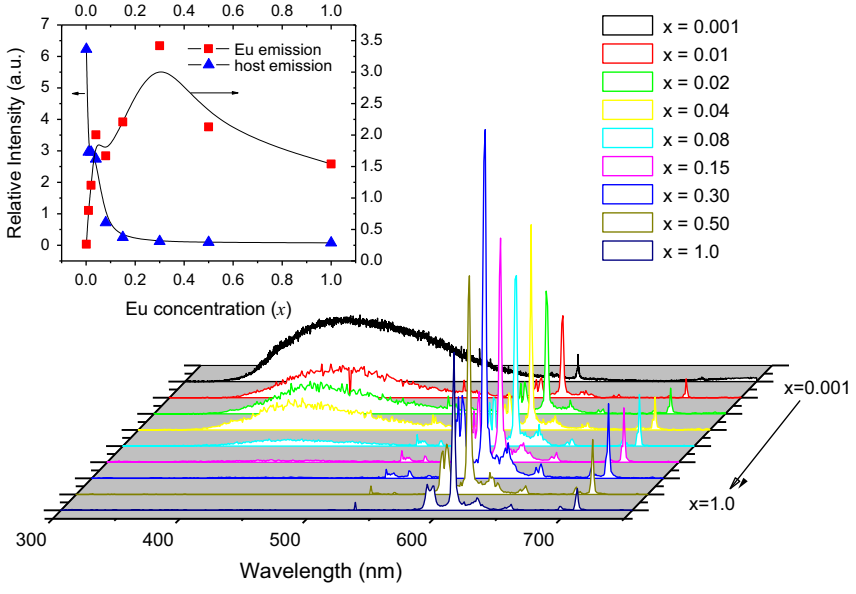

Fig. 4. Emission spectra of $Li_7(La_{3-x}Eu_x)Zr_2O_{12}$ phosphors ($\lambda_{ex}=247$ nm). The inset shows the Eu^{3+} concentration dependence of emission intensity of Eu^{3+} and host.

[21], $N=8$, the critical concentration x_c is about 0.30 in this system. The critical distance R_c is calculated to be 12 Å.

In order to further verify the energy transfer from the host lattice to the Eu^{3+} ions, the emission lifetimes of host emission and Eu^{3+} emission were measured. In Fig. 5 the decay curves of the host luminescence (430 nm) are plotted for different Eu^{3+} concentrations. It is found that when the Eu^{3+} concentration is increased, the decay curve becomes more and more non-exponential and the lifetime of host emission becomes short. The lifetime declines as a function of Eu^{3+} concentration can be attributed to the introduction of extra decay pathways due to the Eu^{3+}-doping: energy transfer from host to Eu^{3+} enhances the host emission decay rate [27]. The presence of Eu^{3+} ions can also be used to explain the different non-exponential behavior at intermediate doping concentrations. At intermediate doping concentrations the Eu^{3+} and the La^{3+} ions are randomly distributed over the RE^{3+} lattice sites. Thus the host environment at different Eu^{3+} doping concentrations is different, which leads to a variety of transfer rates [28].

From the luminescence decay curves in Fig. 5, the energy transfer efficiency can be determined. The energy transfer efficiency from the host to Eu^{3+} ions is defined as the following formula [29]:

$$\eta_T = 1-\frac{\tau}{\tau_0} \tag{3}$$

Based on the average lifetime data derived from Fig. 5 when using Eq. (1), the transfer efficiency is plotted against Eu^{3+}

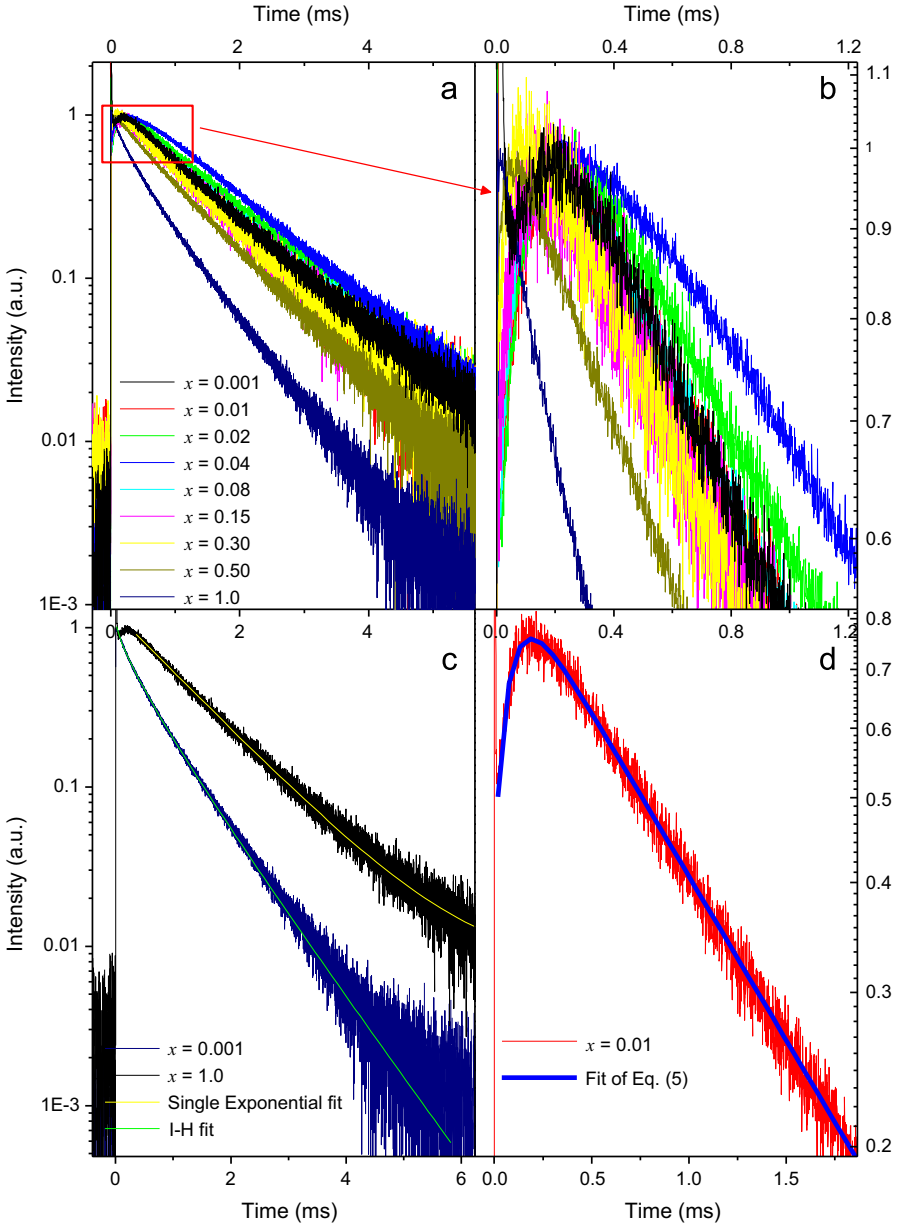

Fig. 6. (a) Decay curves of the Eu^{3+} $^5D_0 \rightarrow {}^7F_2$ luminescence as a function of Eu^{3+} concentration in $Li_7(La_{3-x}Eu_x)Zr_2O_{12}$ phosphors. ($\lambda_{ex}=266$ nm); (b) single exponential fit to the decay curve of $Li_7(La_{2.999}Eu_{0.001})Zr_2O_{12}$ and the I–H model fit to the decay curve of $Li_7(La_{2.0}Eu_{1.0})Zr_2O_{12}$; (c) the enlarged view of zone marked in Fig. 6. (a); and (d) the fit of Eq. (5) for the decay curve of $Li_7(La_{2.99}Eu_{0.01})Zr_2O_{12}$ sample.

concentration in the inset of Fig. 5. When the Eu^{3+} concentration is increased, the transfer efficiency shows an increase up to a maximum value of 60%. As the concentration of Eu^{3+} increases up to 0.30, the energy transfer is close to saturation.

Fig. 6(a) shows the decays curves of Eu^{3+} $^5D_0 \rightarrow {}^7F_2$ luminescence for different Eu^{3+} concentrations. It can be seen that the decay profiles exhibit single exponential for concentrations up to 0.30, and the lifetimes do not change a lot. They can be fitted well with single exponential equation:$I(t) = I_0 + A\exp(-t/\tau)$. The decay time τ of $Li_7(La_{2.999}Eu_{0.001})Zr_2O_{12}$ derived from the fitted curves is close to 1.19 ms [see Fig. 6(b)]. It is also found from Fig. 6(a) that as the Eu^{3+} concentration is further increased, the decay patterns become increasingly non-exponential and the decay time decreases. When the doped concentration is increased, the sample have more and more quenching centers and the non-radiative rate increases, which causes the lifetime to be shortened [30].

It is well known that there are three different regimes of donor decay: no diffusion, diffusion limited decay and fast diffusion. It is found from Fig. 6(b) that the decay of Eu^{3+} in $Li_7(La_{2.0}Eu_{1.0})Zr_2O_{12}$ has an initial fast decay component followed by a more linear, slow decay component. This behavior is a characteristic of diffusion-limited relaxation, which leads us to conclude that this sample diffusion does not play a significant role in the relaxation process [31]. So we apply the direct energy transfer based Inokuti–Hirayama model to analyze the decay curves [32]. This model is satisfactory to describing energy transfer processes in which the donor–acceptor transfer is much faster than the diffusion among the donors. In this model the experimental decay curve can be described as

$$I(t) = I_0 \exp\left[-(t/\tau_s) - (C_A/C_0)\Gamma(1-3/q)(t/\tau_s)^{3/q}\right] \quad (4)$$

In Eq. (4), Γ is the gamma function, C_A is the concentration of acceptors, C_0 is the critical concentration of acceptors, τ_s is the lifetime of the donor in the absence of the acceptor, and $q=6$, 8, or 10 depending on whether the multipolar interaction is dipole–dipole, dipole–quadrupole, or quadrupole–quadrupole, respectively. The critical concentration is defined as $3/(4\pi R_c^3)$, where R_c is the critical distance. A best fit of the decay curve to this equation can be used to determine the type of interaction. In this case, Eu^{3+} is both donor and the acceptor ion. The concentrations used are put in units of the number of ions/cm^3. The donor lifetime τ_s (1.19 ms) is taken from lifetimes of the sample of $x=0.001$. Parameter C_0 is allowed to vary during the fit. The excellent fits of Eq. (4) to the experimental data are achieved when we set $q=6$, and one of the results is shown in Fig. 6(b), which leads us to conclude that the relaxation process occurs via dipole–dipole interaction. The derived value of C_A/C_0 is 0.41. The calculated critical concentration (C_0) and critical distance (R_c) are 9.01×10^{21} ions/cm^3 and 2.97 Å. The value of R_c is in the same order of magnitude but not comparable to that from the concentration quenching data. The discrepancy might be originated from the error of assuming that C_A is equal to Eu^{3+} concentration [33].

Moreover, it is found from Fig. 6(c) that these decay curves exhibit a rising part before decaying, indicating that there is a decaying source feeding this level [27]. The initial buildup process is significantly influenced by Eu^{3+} concentration, which becomes faster and faster with the increasing Eu^{3+} concentration. This is attributed to a faster depopulation of the host donors due to the presence of more Eu^{3+} acceptors [34]. These $^5D_0$ decay curves are well described by a simplified model equation [27]

$$I(t) = \left[I_0 + I_1\left(1-\exp\left(\frac{-t}{\tau_{rs}}\right)\right)\right]\exp\left(\frac{-t}{\tau_{D_0}}\right) \quad (5)$$

where τ_{rs} and τ_{D0} are the rise time and the decay time of the $^5D_0$ level. One of the fitting result ($x=0.01$) is shown in Fig. 6(d). The derived values of τ_{rs} and τ_{D0} are 90 μs and 1.16 ms, respectively. For all samples the derived rise times are longer than the decay times of the host emission. We think that except for the feeding of the Eu^{3+} excited state by energy transfer from host to Eu^{3+}, two possible mechanisms are also possible to populate the $^5D_0$ level. One is the cross relaxation process following the scheme,$(^5D_J \rightarrow {}^5D_0) \rightarrow ({}^7F_0 \rightarrow {}^7F_{J'})$, between Eu^{3+} ions [35,36]; another is the multiphonon process from the higher Eu^{3+} multiplet $^5D_1$[37]. This point is under investigation.

4. Conclusions

In the present work we have reported the luminescence properties of $Li_7(La_{3-x}Eu_x)Zr_2O_{12}$ phosphors. $Li_7La_3Zr_2O_{12}$ host emits blue light under UV excitation. When doped with Eu^{3+}, $Li_7(La_{3-x}Eu_x)Zr_2O_{12}$ phosphors exhibit band emission from host and line emission from Eu^{3+}. The intensity of host emission band decreases as the Eu^{3+} dopants are increased; while the intensity of Eu^{3+} emission increases when Eu^{3+} concentration is up to $x=0.30$. This phenomenon suggests that there exists efficient energy transfer from host to Eu^{3+}. The time-resolved luminescence decay curves of host and Eu^{3+} $^5D_0 \rightarrow {}^7F_2$ luminescence further confirm this kind of energy transfer. The relaxation process between Eu^{3+} ions occurs via dipole–dipole interaction.

Acknowledgments

The project was sponsored by SRF for ROCS, SEM (2011-508), Technology Program of Hunan Provincial Department of Housing and Urban–Rural development (No. 201020), This research was supported by Basic Science Research Program through the National Research Foundation of Korea(NRF) funded by the Ministry of Science, ICT & Future Planning (NRF-2013-R1A1A2009154).

References

[1] S. Shionoya, W.M. Yen, in: Phosphor Handbook, CRC press, New York, 1999.
[2] W.-T. Chen, H.-S. Sheu, R.-S. Liu, J.P. Attfield, Cation-size-mismatch tuning of photoluminescence in oxynitride phosphors, Journal of the American Chemical Society 134 (2012) 8022–8025.
[3] K. Takahashi, K. Yoshimura, M. Harada, Y. Tomomura, T. Takeda, R.J. Xie, N. Hirosaki, On the origin of fine structure in the

photoluminescence spectra of the beta-sialon:Eu^{2+} green phosphor, Science and Technology of Advanced Materials 13 (2012) 015004.
[4] L. Chen, C.C. Lin, C.W. Yeh, R.S. Liu, Light converting inorganic phosphors for white light-emitting diodes, Materials 3 (2010) 2172–2195.
[5] P. Sharma, R. Dutta, A. Pandey, Performance of YAG:Eu^{3+}; YAG:Tb^{3+}; and BAM:Eu^{2+} plasma display nanophosphors, Journal of Nanoparticle Research 14 (2012) 731.
[6] I. Sabikoglu, M. Ayvacikli, A. Bergeron, A. Ege, N. Can, Photoluminescence investigations of Li_2SiO_3:Ln (Ln=Er^{3+}, Eu^{3+}, Dy^{3+}, Sm^{3+}) phosphors, Journal of Luminescence 132 (2012) 1597–1602.
[7] S.T. Mukherjee, V. Sudarsan, P.U. Sastry, A.K. Patra, A.K. Tyagi, Annealing effects on the microstructure of combustion synthesized Eu^{3+} and Tb^{3+} doped Y_2O_3 nanoparticles, Journal of Alloys and Compounds 519 (2012) 9–14.
[8] L. Zeng, W.J. Tang, Synthesis and luminescence properties of Eu^{3+}-activated $NaLa(MoO_4)(WO_4)$ phosphor, Ceramics International 38 (2012) 837–840.
[9] X. Wu, Y. Huang, H.J. Seo, The luminescence spectroscopy and thermal stability of red-emitting phosphor $Ca_9Eu(VO_4)_7$, Ceramics International 37 (2011) 2323–2328.
[10] C. Xu, Y. Li, Y. Huang, Y.M. Yu, H.J. Seo, Luminescence characteristics and site-occupancy of Eu^{2+}- and Eu^{3+}-doped $MgZn_2(PO_4)_2$ phosphors, Journal of Materials Chemistry 22 (2012) 5419–5426.
[11] U. Caldiño, E. Álvarez, A. Speghini, M. Bettinelli, New greenish-yellow and yellowish-green emitting glass phosphors: Tb^{3+}/Eu^{3+} and Ce^{3+}/Tb^{3+}/Eu^{3+} in zinc phosphate glasses, Journal of Luminescence 135 (2013) 216–220.
[12] R. Martinez-Martinez, A. Speghini, M. Bettinelli, C. Falcony, U. Caldino, White light generation through the zinc metaphosphate glass activated by Ce^{3+}, Tb^{3+} and Mn^{2+} ions, Journal of Luminescence 129 (2009) 1276–1280.
[13] Z. Xu, L. He, Z. Tang, R. Mu, X. Cao, Evolution of high temperature corrosion behavior of $La_2(Zr_{0.7}Ce_{0.3})_2O_7$ with the addition of Y_2O_3 thermal barrier coatings in contacts with vanadate-sulfate salts, Journal of Alloys and Compounds 536 (2012) 106–112.
[14] H.S. Soares, X. Zhang, I. Antunes, J.R. Frade, G.C. Mather, D.P. Fagg, Effect of phosphorus additions on the sintering and transport properties of proton conducting $BaZr_{0.85}Y_{0.15}O_{3-\delta}$, Journal of Solid State Chemistry 191 (2012) 27–32.
[15] J. Alarcon, D. Vandervoort, G. Blasse, Efficient Eu^{3+} luminescence in non-lanthanide host lattices, Materials Research Bulletin 27 (1992) 467–472.
[16] V. Singh, S. Watanabe, T.K. Gundu Rao, K. Al-Shamery, M. Haase, Y.-D. Jho, Synthesis, characterisation, luminescence and defect centres in solution combustion synthesised $CaZrO_3$:Tb^{3+} phosphor, Journal of Luminescence 132 (2012) 2036–2042.
[17] G. Blasse, G. Bernardi, D.J.W. Ijdo, J.R. Plaisier, Yellow zirconate luminecence in $Ca_3ZrSi_2O_9$,, Journal of Alloys and Compounds 217 (1995) 29–30.
[18] L. Zhang, G.Y. Hong, X.L. Sun, The Luminescence of the phosphor Sr_2ZrO_4 with one-dimensional chains structure, Chinese Chemical Letters 10 (1999) 799–802.
[19] L. Shi, H.J. Seo, Tunable white-light emission in single-phased $K_2Y_{1-x}Eu_xZr(PO_4)_3$ phosphor, Optics Express 19 (2011) 7147–7152.
[20] H. Buschmann, J. Dolle, S. Berendts, A. Kuhn, P. Bottke, M. Wilkening, P. Heitjans, A. Senyshyn, H. Ehrenberg, A. Lotnyk, V. Duppel, L. Kienle, J. Janek, Structure and dynamics of the fast lithium ion conductor $Li_7La_3Zr_2O_{12}$, Physical Chemistry Chemical Physics 13 (2011) 19378–19392.
[21] J. Tan, A. Tiwari, Synthesis of cubic phase $Li_7La_3Zr_2O_{12}$ electrolyte for solid-state lithium-ion batteries, Electrochemical and Solid-State Letters 15 (2012) A37–A39.
[22] L. Li, S.H. Zhou, S.Y. Zhang, Investigation on charge transfer bands of Ce^{4+} in Sr_2CeO_4 blue phosphor, Chemical Physics Letters 453 (2008) 283–289.
[23] Y. Takahashi, K. Kitamura, N. Iyi, S. Inoue, Visible orange photoluminescence in a barium titanosilicate $BaTiSi_2O_7$, Applied Physics Letters 88 (2006) 151903.
[24] N. Xie, J.Y. Liu, Y.L. Huang, S.I. Kim, H.J. Seo, Tunable luminescence properties and efficient energy transfer in Eu^{2+},Mn^{2+} co-doped $Ba_2MgP_4O_{13}$, Ceramics International 38 (2012) 1489–1495.
[25] G. Blasse, B.C. Grabmaier, Luminescent Materials, Springer, Berlin etc, 1994.
[26] G. Blasse, Energy transfer in oxidic phosphors, Philips Research Reports 24 (1969) 131–144.
[27] M.L. Debasu, D. Ananias, A.G. Macedo, J. Rocha, L.D. Carlos, Emission-decay curves, energy-transfer and effective-refractive index in Gd_2O_3:Eu^{3+} nanorods, Journal of Physical Chemistry C, 115, 15297–15303.
[28] P. Vergeer, T.J.H. Vlugt, M.H.F. Kox, M.I. den Hertog, J.P.J.M. van der Eerden, A. Meijerink, Quantum cutting by cooperative energy transfer in $Yb_xY_{1-x}PO_4$:Tb^{3+}, Physical Review B 71 (2005) 014119.
[29] S.C. Jang, Y.C. Shu, F.S. Chuang, W.C. Tsen, J.D. Chow, C.C. Chen, The dispersants effect on physical properties of long-lasting luminescent polypropylene, Journal of Applied Polymer Science 124 (2012) 4645–4654.
[30] S.H. Huang, D. Wang, Y. Wang, L.Z. Wang, X. Zhang, P.P. Yang, Self-assembled three-dimensional $NaY(WO_4)_2$:Ln^{3+} architectures: hydrothermal synthesis, growth mechanism and luminescence properties, Journal of Alloys and Compounds 529 (2012) 140–147.
[31] J. Collins, M. Geen, M. Bettinelli, B. Di Bartolo, Dependence of cross-relaxation on temperature and concentration from the $^1D_2$ level of Pr^{3+} in YPO_4, Journal of Luminescence 132 (2012) 2626–2633.
[32] M. Inokuti, F. Hirayama, Influence of energy transfer by eechange mechanism on donor luminescence, Journal of Chemical Physics 43 (1965) 1978–1989.
[33] K.S. Sohn, Y.G. Choi, Y.Y. Choi, H.D. Park, Energy transfer between Tb^{3+} ions in $YAlO_3$ host, Journal of the Electrochemical Society 147 (2000) 3552–3558.
[34] C. Zhang, H. Liang, S. Zhang, C. Liu, D. Hou, L. Zhou, G. Zhang, J. Shi, Efficient sensitization of Eu^{3+} emission by Tb^{3+} in $Ba_3La(PO_4)_3$ under VUV–UV excitation: energy transfer and tunable emission, Journal of Physical Chemistry C 116 (2012) 15932–15937.
[35] E. Zych, D. Hreniak, W. Strek, Spectroscopic properties of Lu_2O_3/Eu^{3+} nanocrystalline powders and sintered ceramics, Journal of Physical Chemistry B 106 (2002) 3805–3812.
[36] X. Zhang, H.J. Seo, Photoluminescence and concentration quenching of $NaCa_4(BO_3)_3$:Eu^{3+} phosphor, Journal of Alloys and Compounds 503 (2010) L14–L17.
[37] K.H. Jang, W.K. Sung, E.S. Kim, L. Shi, J.H. Jeong, H.J. Seo, Time-resolved luminescence spectroscopy of a YVO_4:Eu^{3+} thin film, Journal of Luminescence 129 (2009) 1853–1856.